NUCL SCI TECH (2016) 27:56
DOI 10.1007/s41365-016-0067-9

Synchrotron FTIR spectroscopy reveals molecular changes in *Escherichia coli* upon Cu^{2+} exposure

Xiao-Juan Hu[1,2] · Zhi-Xiao Liu[1,2] · Ya-Di Wang[1,2] · Xue-Ling Li[3,4] · Jun Hu[1] · Jun-Hong Lü[1]

Received: 27 December 2015 / Revised: 28 March 2016 / Accepted: 1 April 2016 / Published online: 9 May 2016

Abstract Copper ions (e.g., Cu^{2+}) have outstanding antibacterial properties, but the exact mechanism is rather complex and not fully understood. In this work, synchrotron Fourier transform infrared (FTIR) spectroscopy was used as an analytical tool to investigate the $CuCl_2$-induced biochemical changes in *Escherichia coli*. Our spectral measurements indicated that this technique is sensitive enough to detect changes in membrane lipids, nucleic acids, peptidoglycans and proteins of Cu^{2+}-treated bacteria. Interestingly, for short-time treated cells, the effects on phospholipid composition were clearly shown, while no significant alterations of proteins, nucleic acids and peptidoglycans were found. PeakForce quantitative nano-mechanics mode atomic force microscopy (AFM) confirmed the changes in the topography and mechanical properties of bacteria upon the Cu^{2+} exposure. This study demonstrated that FTIR spectroscopy combined with AFM can provide more comprehensive evaluation on the biochemical and mechanical responses of bacteria to copper.

Keywords Copper ions · Antibacterial effect · *Escherichia coli* · Synchrotron FTIR spectroscopy · Atomic force microscopy

1 Introduction

Copper, accredited to its antimicrobial properties, has been empirically utilized for more than 10,000 years and received renewed scientific interest in the last decades for its application potential in the modern healthcare setting [1]. However, the exact antibacterial mechanisms of copper are rather complex and not properly understood, although some possible modes of action have been put forward [2].

Current biochemical and molecular evidence indicated that the action of copper ions on bacterial cells is multifactorial rather than aims at one target [3, 4]. Copper ions not only act as a catalyst to generate reactive oxygen species (ROS), which cause oxidative damage to proteins, lipids and nucleic acids [5–8], but also inactive proteins through replacing other metal ions binding sites on proteins or affect the metabolism by damaging Fe–S clusters in enzymes [9]. In addition, the membrane as a key target for the antimicrobial action of copper had been proposed [5, 10–13]. Transmission electron microscopy (TEM) or AFM observation confirmed that copper can indeed induce the

Supported by National Natural Science Foundation of China (No. 11474298), Shanghai Pujiang Program (No. 13PJ1410500), Special Funds for Enterprise Independent Innovation of Shanghai (CXY-2013-58) and Hundred Talents Program of the Chinese Academy Sciences.

Electronic supplementary material The online version of this article (doi:10.1007/s41365-016-0067-9) contains supplementary material, which is available to authorized users.

✉ Jun-Hong Lü
lujunhong@sinap.ac.cn

[1] Division of Physical Biology and CAS Key Laboratory of Interfacial Physics and Technology, Shanghai Institute of Applied Physics, Chinese Academy of Sciences, Shanghai 201800, China

[2] University of Chinese Academy of Sciences, Beijing 100049, China

[3] Shanghai Center for Bioinformation Technology, Shanghai Academy of Science and Technology, Shanghai 201203, China

[4] Center for Clinical and Translational Medicine, Shanghai Industrial Technology Institute, Shanghai 201203, China

membrane surface damages. However, few studies were performed on the changes in cellular components and mechanical properties after bacteria were exposed to copper ions.

FTIR spectroscopy is a powerful tool to rapidly, non-destructively detect the chemical compositions of the biological samples [14]. Recently, it has been widely used in microbiology, particularly applied to study the molecular changes in microorganisms in the stress conditions [15]. For instance, the responses of *E. Coli* when subjected to heat, cold as well as ethanol and the interaction between bacteria and metals (e.g., Ag^{+}, Zn^{2+}, Fe_2O_3 and TiO_2) were investigated by ATR-sFTIR [16–18].

In this study, *E. coli* was chosen as the representative of gram-negative bacterium to study the changes in cellular components along with time caused by copper ions through FTIR spectroscopy. To rule out the heterogeneity of bacterial cells among their biochemical compositions and their response to stress conditions [19], the average spectra of tens cells were measured and analyzed. In addition, the morphological and mechanical properties changes in *E. coli* induced by copper were simultaneously evaluated by using a novel mode of AFM based on PeakForce quantitative nano-mechanics (PF-QNM) measurement [20].

2 Materials and methods

2.1 Bacterial strain and growth conditions

Escherichia coli DH5 α strain was inoculated into 3 mL Luria–Bertani broth and incubated overnight at 37 °C with continuous shaking (120 rpm, Qiangle HYL-C) until stationary growth phase. This preculture was then diluted to a concentration of approximately 10^8 CFU/mL for the following experiments.

2.2 Copper ions solutions

$CuCl_2$ powder was dissolved into ultra-pure water (18.2 MΩ, USF-ELGA Maxima water purification system) to obtain a concentrated solution of copper ions (1 M) and then further diluted into the final concentration 6 mM [12].

2.3 Exposure of *E. coli* to copper ions

After exposed to 6 mM $CuCl_2$ for 0, 20, 40 and 60 min, respectively, *E. coli* cells were collected by centrifugation (10,000 rpm, 1 min) and washed three times with sterile saline solution (0.9 % NaCl). The bacterial number (CFU/mL) was counted after the harvested cells were plated on LB agar medium at 37 °C for 24 h.

2.4 Synchrotron FTIR spectroscopy of *E. coli*

FTIR spectroscopy experiments were performed at the beamline BL01B1 of the Shanghai Synchrotron Radiation Facility (SSRF) as the following procedure: $CuCl_2$-exposed bacterial cells were harvested at 0, 20, 40 and 60 min by centrifugation (10,000 rpm, 1 min) and washed five times to remove any medium. Prior to the FTIR measurement, one drop of harvested cells was deposited on the BaF_2 window and left to dry at room temperature. The absorbance spectra were collected by Nicolet 6700 FTIR spectrometer with Nicolet Continuum IR Microscope with an aperture of 20 × 20 μm. For each sample at different exposed time, 15 small clusters were measured within the range of 4000–800 cm^{-1} with 256 co-added scans at 4 cm^{-1} resolution at room temperature. Raw spectra were baseline corrected and smoothed by 13-point Savitzky–Golay method. The second derivative was calculated to enhance the spectral resolution. Data were collected and analyzed by OMIC 9 (Thermo). To test the significance of the differences among the samples, hypothesis testing two-sample *t* test was performed on the groups. Analysis was made by OriginPro 8.

2.5 PeakForce quantitative nano-mechanics (PF-QNM) measurements of bacterial cells

AFM measurements were taken at room temperature in deionized water using the PF-QNM mode on a Bruker Multimode 8 SPM. Polyethyleneimine (PEI)-coated glasses, which provided positive charge surfaces for bacterial adhesion, were used to immobilize cells [21, 22]. V-shaped silicon nitride cantilevers with a spring constant of 0.35 N/m were used in all the measurements. All images were recorded at 256 pixels × 256 pixels with an applied force of 6 nN, peak force frequency were set at 2 kHz and scan rate at 1 Hz. Image analysis was performed on NanoScope offline processing system.

3 Results and discussion

The survival curve of the *E. coli* exposed to copper ions (Fig. 1) indicated that 6 mM $CuCl_2$ has a significant effect on the bacterial survival. To investigate the changes in cellular components during this process, FTIR spectroscopy was performed on the cells with the exposure time 0, 20, 40 and 60 min, respectively.

A representative FTIR spectrum of *E. coli* in the region of 4000–800 cm^{-1} is displayed in Fig. 2. According to the

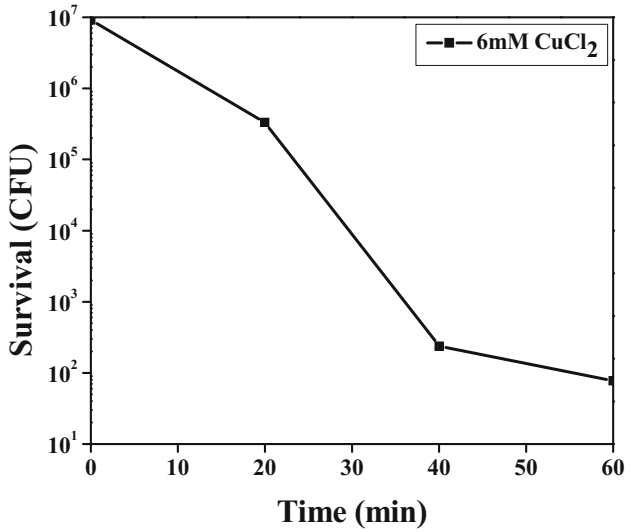

Fig. 1 *Escherichia coli* survival curve following exposure to 6 mM $CuCl_2$ in LB medium

references, the regions 3000–2800 and 1480–1300 cm^{-1} are assigned to fatty acids which mostly encountered in cell membranes. The regions 1760–1600 and 1600–1480 cm^{-1} are representative of amide I and amide II bands, respectively. The amide I adsorption is mainly from C=O stretching of proteins, and amide II adsorption is assigned to N–H bending vibration and C–N stretching vibration of proteins. The region from 1350 to 1000 cm^{-1} represents PO_2 asymmetric stretching of mainly nucleic acids and phospholipids [19], while sugars exhibit strong bands in this region due to C–O–C and P–O–C vibrations [23].

In our experiments, the changes in the spectra regions caused by copper treatment were analyzed. To eliminate the interference of baseline as well as the other background and to improve the sensitivity and resolution, second-derivative spectra were used (Figs. S1, 2). As shown in Fig. 3 and Table 1, Cu^{2+} exposure caused kinds of shifts in the second-derivative spectra. For example, in the fatty acid regions (3000–2800 and 1480–1340 cm^{-1}) (Fig. 3a), the wavenumbers 1453 and 1392 cm^{-1} shifted to higher energies dramatically ($p < 0.05$) after 20-min exposure (Table 1), corresponding to the asymmetric CH_2 bending and the symmetric COO^- stretching [24–27], meaning that the conformation or structure of lipids in the cells had changed [28]. These results suggested that Cu^{2+} had influences on the structure of lipid molecules in the early period of exposure, providing direct evidence that membrane lipids were targets of copper ions [3], while in the amide I and amide II regions (1760–1480 cm^{-1}) (Fig. 3b), wavenumbers of 1659, 1639 and 1547 cm^{-1}, corresponding to C=O stretching, N–H bending and C–N stretching of proteins [29–32], had no dramatically shift ($p < 0.05$) until 40-min exposure (Table 1). Generally, wavenumbers of 1659 and 1547 were assigned to α-helical conformation, while wavenumber of 1639 was attributed to β-sheet [33]. As seen from Table 1, copper treatment induced α-helical bands shift to higher frequencies. These shifts might result from the influences on H-bonding in amide groups and/or the metal binding with amide groups in cellular proteins [25]. These changes suggested that the protein secondary structure was damaged in 40 min after exposed to $CuCl_2$ [34]. In addition, in the second-derivative spectra of nucleic acids and sugars regions (1350–1000 cm^{-1}) (Fig. 3c), wavenumbers of 1242 and 1082 cm^{-1} were assigned to PO_2 asymmetric and symmetric stretching, which were mainly from nucleic acids, and the contribution from phospholipids was negligible [24]. Wavenumbers of 1120 and 1059 cm^{-1} were assigned to symmetric CC stretching of ribose and symmetric C–O–C, P–O–C stretching of polysaccharides on capsule and peptidoglycan, respectively [30, 35–37]. They all shifted to lower frequencies dramatically ($p < 0.05$) after 40-min exposure

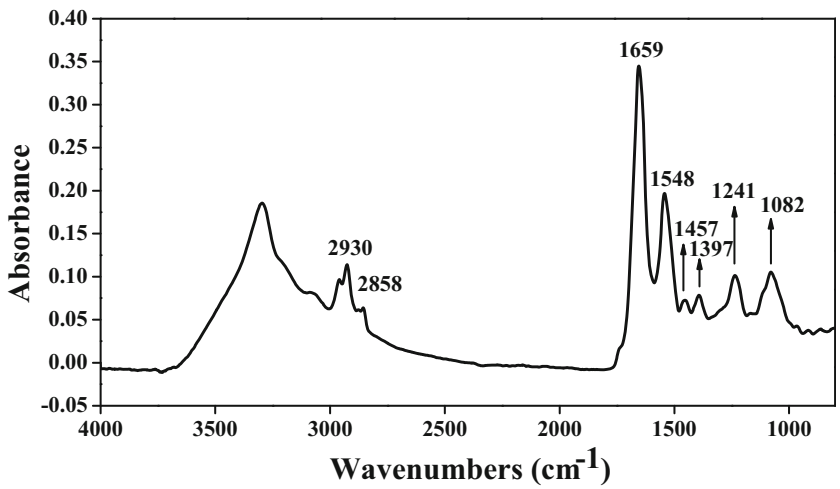

Fig. 2 Representative FTIR absorption spectrum of *E. coli* in the region of 4000–800 cm^{-1}

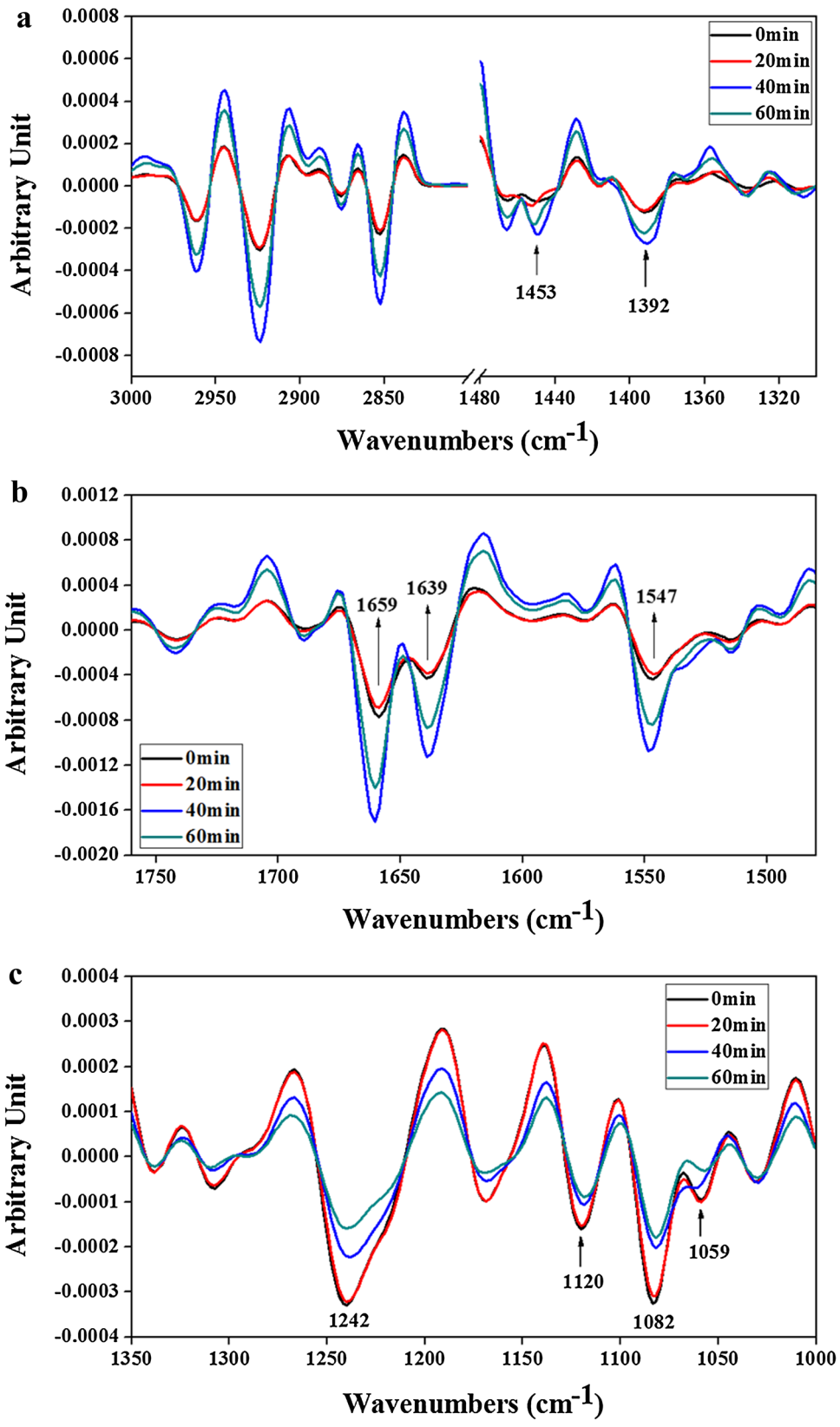

Fig. 3 Second derivative of FTIR spectra of *E. coli* exposed to 6 mM $CuCl_2$ for 0 min (1); 20 min (2); 40 min (3); and 60 min (4). The fatty acid regions (**a**) (3000–2800 and 1480–1340 cm^{-1}), the protein regions (**b**) (1760–1480 cm^{-1}) and the nucleic acids and sugars regions (**c**) (1350–1000 cm^{-1}) were focused, respectively. The peaks were indicated by *arrows*

Table 1 Wavenumber values of the infrared bands of *E. coli* exposed to 6 mM $CuCl_2$ for 0, 20, 40 and 60 min

Functional groups	Wavenumber (cm^{-1})			
	0 min (n = 15)	20 min (n = 15)	40 min (n = 15)	60 min (n = 15)
Amide I	1659.15 ± 0.28	1659.25 ± 0.32↑	1660.42 ± 0.9*↑	1659.99 ± 0.74*↑
	1639.37 ± 0.26	1639.22 ± 0.40↓	1638.75 ± 0.18*↓	1638.55 ± 0.22*↓
Amide II	1546.77 ± 0.57	1546.55 ± 0.38↓	1548.24 ± 0.35*↑	1547.92 ± 0.52*↑
CH_2 bending	1452.81 ± 1.23	1454.47 ± 0.40*↑	1453.38 ± 0.27↑	1454.14 ± 0.53*↑
COO^- stretching	1391.59 ± 0.35	1392.78 ± 0.82*↑	1392.13 ± 0.36*↑	1392.69 ± 0.76*↑
PO_2 asymmetric stretching	1241.68 ± 1.28	1241.16 ± 1.04↓	1240.59 ± 0.56*↓	1240.32 ± 0.70*↓
PO_2 symmetric stretching	1082.44 ± 0.57	1082.15 ± 0.49↓	1082.05 ± 0.36*↓	1081.74 ± 0.35*↓
CC symmetric stretching	1119.68 ± 0.65	1119.33 ± 0.80↓	1119.13 ± 0.39*↓	1118.88 ± 0.70*↓
C–O–C, P–O–P stretching	1059.27 ± 0.76	1059.11 ± 0.96↓	1058.65 ± 0.42*↓	1057.71 ± 0.79*↓

The values are the mean ± SD for each group. Comparisons were done by hypothesis testing two-sample *t* test

* The degree of significance was denoted as: $p < 0.05$

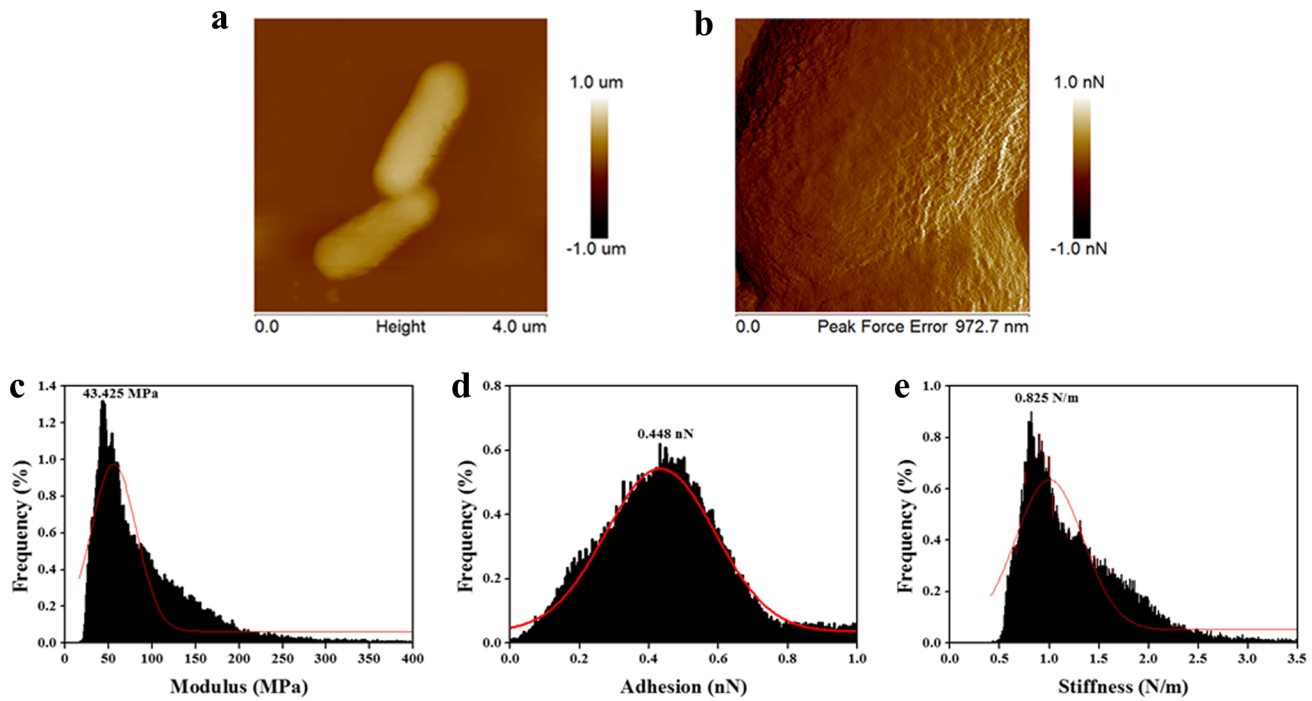

Fig. 4 AFM images of *E. coli*. **a** Height image; **b** high-resolution PeakForce error image; **c** histogram of modulus; **d** histogram of adhesion; **e** histogram of stiffness. Histograms of **c**, **d** and **e** correspond to the *zoom area* of image **b**

(Table 1). The frequencies of PO_2 stretching of nucleic acids at 1242 and 1082 cm^{-1} were significantly lower; these changes could be the products of increased hydration of phosphate moieties, which may be due to metal binding. In previous study, it had been reported that Co^{2+} and Zn^{2+} could induce similar effect [25]. Changes in symmetric CC stretching of ribose might be the results of a modification affecting ribose [28]. Peptidoglycan layer was generally considered to play a dominant role for ionic exchanging and could absorb a lot of counterions from the aqueous environment [38]. It had also been reported that the conductivity of periplasmic space reduced in the present of copper ions [39]. Our results showed that symmetric C–O–C, P–O–C stretching of peptidoglycan shifted to lower frequencies dramatically ($p < 0.05$), indicating an alteration in peptidoglycan structure. We supposed that the damage to peptidoglycan structure might play an important role in the conductivity reducing, which further resulted in the function disorder of *E. coli*. Overall, the FTIR results indicated that $CuCl_2$ could affect bacterial membrane

lipids, proteins, DNA and peptidoglycan, supporting the hypothesis that the actions of copper ions are multifactorial.

It should be noted that copper ions seemed to affect the lipid components in bacteria first. Upon $CuCl_2$ exposure, amide I and amide II bands and peaks in nucleic acids as well as sugars regions did not shift dramatically until 40 min, while the wavenumbers in lipid regions have already changed in 20 min. Based on the fact that a low rate of killing occurred in 20 min (Fig. 2), we assumed the early killing events might be accompanied by the changes in lipids, then protein oxidization [40] and DNA degrade [11].

To further evaluate the effects of Cu^{2+} on bacterial cells, high-resolution imaging and mechanical measurement were carried out using PF-QNM mode AFM (Fig. 4). The results showed that untreated *E. coli* cells had a smooth and featureless surface morphology (Fig. 4a, b) and the modulus varied from 0 to 120 MPa, with a peak value at 43.425 MPa (Fig. 4c). The adhesion force and the stiffness value varied from 0 to 0.8 nN (peak value at 0.448 nN) and from 0.5 to 2.0 N m^{-1} (peak value at 0.825 N m^{-1}), respectively.

However, after exposed to 6 mM $CuCl_2$, the surface morphology of *E. coli* changed seriously (Fig. 5a, e), becoming uneven and exhibited protrusions along with time. The range of modulus, adhesion and stiffness of bacteria are shown in Fig. S3, and the peak values are shown in Fig. 6, respectively. The results showed that the $CuCl_2$ exposure obviously changed cells' modulus, adhesion force and stiffness. Both the modulus and stiffness of *E. coli* decreased along with time. We assumed that the cell softening after $CuCl_2$ exposure might be related to the changes in lipids as indicated in the FTIR results. Interestingly, the adhesion of cells surfaces increased first and then started to decrease after 20 min. Because the adhesion

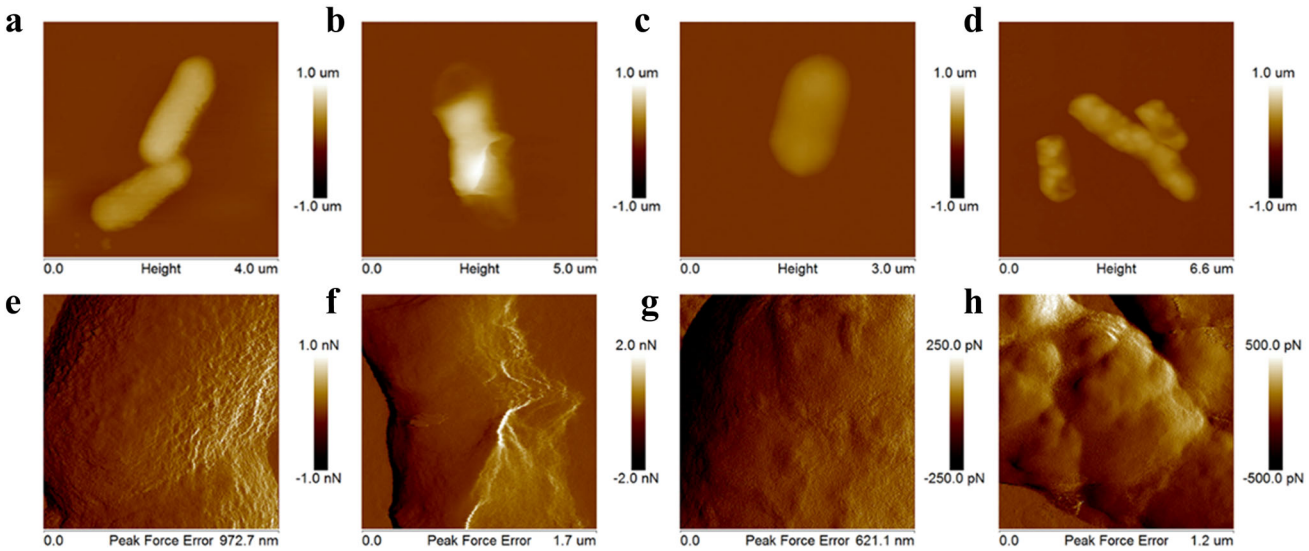

Fig. 5 AFM height images (**a**–**d**) and high-resolution peak force error images (**e**–**h**) of *E. coli* exposed to 6 mM $CuCl_2$ for 0 min (**a**, **e**), 20 min (**b**, **f**), 40 min (**c**, **g**) and 60 min (**d**, **h**)

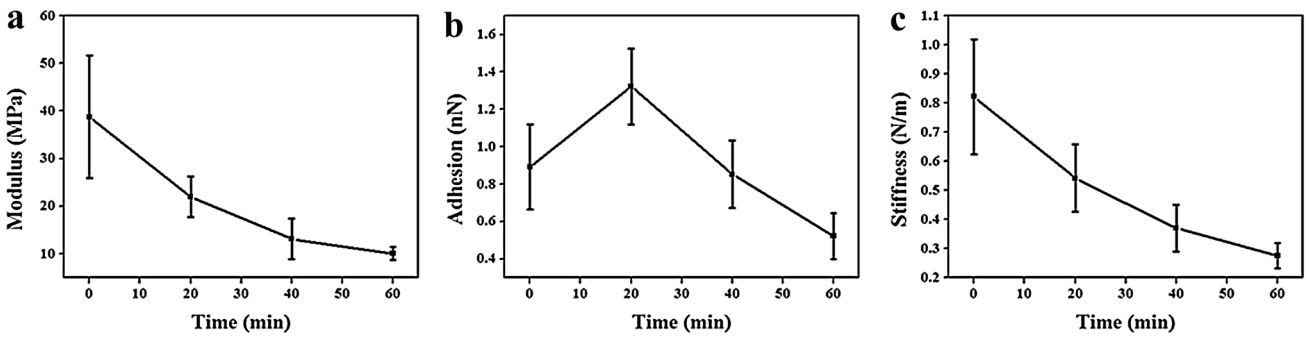

Fig. 6 The peak values of mechanical properties of *E. coli* exposed to 6 mM $CuCl_2$ at different time intervals. **a** Modulus; **b** adhesion; and **c** stiffness. The *error bars* show the standard deviations of five cells in each condition

events were ascribed to the stretching of extracellular substances with the AFM tip [41], the adhesion force changes would be attributed to the changes in cell surface components. Although FTIR results showed that the lipids and polysaccharides have changed in the early period of exposure, whether and how the lipid changes resulted in the adhesion force increase and then polysaccharides led to adhesion force decrease still need more experiments.

4 Conclusion

This study demonstrated the effects of copper ions on the model bacterium *E. coli* using synchrotron FTIR spectroscopy combined with PF-QNM mode AFM. FTIR spectroscopy revealed the changes in cellular components of bacteria induced by copper ions. The results provided evidences that copper ions targeted against several components of bacteria cells, including lipids, proteins, nucleic acids and peptidoglycans. Interestingly, spectral analysis further showed that the effects on phospholipids composition were clearly shown at the short-time treated cells, while no significant alteration of proteins, nucleic acids and peptidoglycans was detected. Atomic force microscopy confirmed the changes in that topography and mechanical properties upon the Cu^{2+} exposure. This study demonstrated that the combination of FTIR spectroscopy and AFM images might provide more comprehensive technique to investigate the biochemical and mechanical response of bacteria to copper.

Acknowledgments We thank the staff of BL01B beamline at National Center for Protein Sciences Shanghai and Shanghai Synchrotron Radiation Facility for assistance during data collection.

References

1. J. O'Gorman, H. Humphreys, Application of copper to prevent and control infection. Where are we now? J. Hosp. Infect. **81**, 217–223 (2012). doi:10.1016/j.jhin.2012.05.009
2. L. Nan, W.C. Yang, Y.Q. Liu et al., Antibacterial mechanism of copper-bearing antibacterial stainless steel against *E. coli*. J. Mater. Sci. Technol. **24**, 197–201 (2008)
3. S.L. Warnes, V. Caves, C.W. Keevil, Mechanism of copper surface toxicity in *Escherichia coli* O157:H7 and Salmonella involves immediate membrane depolarization followed by slower rate of DNA destruction which differs from that observed for gram-positive bacteria. Environ. Microbiol. **14**, 1730–1743 (2012). doi:10.1111/j.1462-2920.2011.02677.x
4. T.P. Dasari, K. Pathakoti, H.-M. Hwang, Determination of the mechanism of photoinduced toxicity of selected metal oxide nanoparticles (ZnO, CuO, Co_3O_4 and TiO_2) to *E. coli* bacteria. J. Environ. Sci. (China) **25**, 882–888 (2013). doi:10.1016/s1001-0742(12)60152-1
5. C. Espirito Santo, E.W. Lam, C.G. Elowsky et al., Bacterial killing by dry metallic copper surfaces. Appl. Environ. Microbiol. **77**, 794–802 (2011). doi:10.1128/aem.01599-10
6. S.L. Warnes, S.M. Green, H.T. Michels et al., Biocidal efficacy of copper alloys against *Pathogenic Enterococci* involves degradation of genomic and plasmid DNAs. Appl. Environ. Microbiol. **76**, 5390–5401 (2010). doi:10.1128/aem.03050-09
7. S.L. Warnes, C.W. Keevil, Mechanism of copper surface toxicity in vancomycin-resistant *Enterococci* following wet or dry surface contact. Appl. Environ. Microbiol. **77**, 6049–6059 (2011). doi:10.1128/aem.00597-11
8. R.N.N. Abskharon, S.H.A. Hassan, M.H. Kabir et al., The role of antioxidants enzymes of *E. coli* ASU3, a tolerant strain to heavy metals toxicity, in combating oxidative stress of copper. World J. Microbiol. Biotechnol. **26**, 241–247 (2010). doi:10.1007/s11274-009-0166-4
9. L. Macomber, J.A. Imlay, The iron–sulfur clusters of dehydratases are primary intracellular targets of copper toxicity. Proc. Natl. Acad. Sci. U.S.A. **106**, 8344–8349 (2009). doi:10.1073/pnas.0812808106
10. D. Quaranta, T. Krans, C.E. Santo et al., Mechanisms of contact-mediated killing of yeast cells on dry metallic copper surfaces. Appl. Environ. Microbiol. **77**, 416–426 (2011). doi:10.1128/aem.01704-10
11. C.E. Santo, D. Quaranta, G. Grass, Antimicrobial metallic copper surfaces kill *Staphylococcus haemolyticus* via membrane damage. Microbiologyopen **1**, 46–52 (2012). doi:10.1002/mbo3.2
12. R. Hong, T.Y. Kang, C.A. Michels et al., Membrane lipid peroxidation in copper alloy-mediated contact killing of *Escherichia coli*. Appl. Environ. Microbiol. **78**, 1776–1784 (2012). doi:10.1128/aem.07068-11
13. S.I. Volentini, R.N. Farias, L. Rodriguez-Montelongo et al., Cu(II)-reduction by *Escherichia coli* cells is dependent on respiratory chain components. Biometals **24**, 827–835 (2011). doi:10.1007/s10534-011-9436-3
14. S. Ling, Z. Qi, D. Knight et al., Synchrotron FTIR microspectroscopy of single natural silk fibers. Biomacromolecules **12**, 3344–3349 (2011). doi:10.1021/bm2006032
15. A. Alvarez-Ordonez, D.J.M. Mouwen, M. Lopez et al., Fourier transform infrared spectroscopy as a tool to characterize molecular composition and stress response in foodborne pathogenic bacteria. J. Microbiol. Methods **84**, 369–378 (2011). doi:10.1016/j.mimet.2011.01.009
16. S.J. Parikh, J. Chorover, ATR-FTIR spectroscopy reveals bond formation during bacterial adhesion to iron oxide. Langmuir **22**, 8492–8500 (2006). doi:10.1021/la061359p
17. J. Kiwi, V. Nadtochenko, Evidence for the mechanism of photocatalytic degradation of the bacterial wall membrane at the TiO_2 Interface by ATR-FTIR and laser kinetic spectroscopy. Langmuir **21**, 4631–4641 (2005). doi:10.1021/la046983l
18. T. Jan, J. Iqbal, M. Ismail et al., Eradication of multi-drug resistant bacteria by Ni doped ZnO nanorods: structural, raman and optical characteristics. Appl. Surf. Sci. **308**, 75–81 (2014). doi:10.1016/j.apsusc.2014.04.100
19. C. Saulou, F. Jamme, L. Girbal et al., Synchrotron FTIR microspectroscopy of *Escherichia coli* at single-cell scale under silver-induced stress conditions. Anal. Bioanal. Chem. **405**, 2685–2697 (2013). doi:10.1007/s00216-013-6725-4
20. B. Zhao, Y. Song, S. Wang et al., Mechanical mapping of nanobubbles by PeakForce atomic force microscopy. Soft Matter **9**, 8837–8843 (2013). doi:10.1039/c3sm50942g
21. D. Alsteens, H. Trabelsi, P. Soumillion et al., Multiparametric atomic force microscopy imaging of single bacteriophages extruding from living bacteria. Nat. Commun. **4**, 2926 (2013). doi:10.1038/ncomms3926

22. V. Vadillo-Rodrigues, H.J. Busscher, W. Norde et al., Comparison of atomic force microscopy interaction forces between bacteria and silicon nitride substrata for three commonly used immobilization methods. Appl. Environ. Microbiol. **70**, 5441–5446 (2004). doi:10.1128/aem.70.9.5441-5446.2004
23. S. Kaminskyj, K. Jilkine, A. Szeghalmi et al., High spatial resolution analysis of fungal cell biochemistry–bridging the analytical gap using synchrotron FTIR spectromicroscopy. FEMS Microbiol. Lett. **284**, 1–8 (2008). doi:10.1111/j.1574-6968.2008.01162.x
24. G. Cakmak, I. Togan, F. Severcan, 17 beta-estradiol induced compositional, structural and functional changes in rainbow trout liver, revealed by FT-IR spectroscopy: a comparative study with nonylphenol. Aquat. Toxicol. **77**, 53–63 (2006). doi:10.1016/j.aquatox.2005.10.015
25. A.A. Kamnev, FTIR spectroscopic studies of bacterial cellular responses to environmental factors, plant-bacterial interactions and signalling. Spectrosc. Int. J. **22**, 83–95 (2008). doi:10.3233/spe-2008-0329
26. M. Jackson, B. Ramjiawan, M. Hewko et al., Infrared microscopic functional group mapping and spectral clustering analysis of hypercholesterolemic rabbit liver. Cell. Mol. Biol. **44**, 89–98 (1998)
27. D. Naumann, FT-infrared and FT-Raman spectroscopy in biomedical research. Appl. Spectrosc. Rev. **24**, 323–377 (2001). doi:10.1081/ASR-100106157
28. M. Kardas, A.G. Gozen, F. Severcan, FTIR spectroscopy offers hints towards widespread molecular changes in cobalt-acclimated freshwater bacteria. Aquat. Toxicol. **155**, 15–23 (2014). doi:10.1016/j.aquatox.2014.05.027
29. P.I. Haris, F. Severcan, FTIR spectroscopic characterization of protein structure in aqueous and non-aqueous media. J. Mol. Catal. B Enzym. **7**, 207–221 (1999). doi:10.1016/s1381-1177(99)00030-2
30. N.S. Ozek, I.B. Bal, Y. Sara et al., Structural and functional characterization of simvastatin-induced myotoxicity in different skeletal muscles. Biochim. Biophys. Acta Gen. Subj. **1840**, 406–415 (2014). doi:10.1016/j.bbagen.2013.09.010
31. J. Kong, S. Yu, Fourier transform infrared spectroscopic analysis of protein secondary structures. Acta Biochim. Biophys. Sin. **39**, 549–559 (2007). doi:10.1111/j.1745-7270.2007.00320.x
32. A.M. Dwivedi, S. Krimm, Vibrational analysis of peptides, polypeptides, and proteins. 18. Conformational sensitivity of the alpha-helix spectrum-alpha-I-poly (L-alanine) and alpha-II-poly (L-alanine). Biopolymers **23**, 923–943 (1984). doi:10.1002/bip.360230509
33. S.J. Ling, Z.M. Qi, D.P. Knight et al., Insight into the structure of single *Antheraea pernyi* silkworm fibers using synchrotron FTIR microspectroscopy. Biomacromolecules **14**, 1885–1892 (2013). doi:10.1021/bm400267m
34. P. Heraud, E.S. Ng, S. Caine et al., Fourier transform infrared microspectroscopy identifies early lineage commitment in differentiating human embryonic stem cells. Stem Cell Res. **4**, 140–147 (2010). doi:10.1016/j.scr.2009.11.002
35. K. Maquelin, C. Kirschner, L.P. Choo-Smith et al., Identification of medically relevant microorganisms by vibrational spectroscopy. J. Microbiol. Methods **51**, 255–271 (2002). doi:10.1016/s0167-7012(02)00127-6
36. M. Banyay, M. Sarkar, A. Graslund, A library of IR bands of nucleic acids in solution. Biophys. Chem. **104**, 477–488 (2003). doi:10.1016/s0301-4622(03)00035-8
37. F. Quiles, F. Humbert, A. Delille, Analysis of changes in attenuated total reflection FTIR fingerprints of *Pseudomonas fluorescens* from planktonic state to nascent biofilm state. Spectrochim. Acta Part A **75**, 610–616 (2010). doi:10.1016/j.saa.2009.11.026
38. B.D. Hoyle, T.J. Beveridge, Metal-binding by the peptidoglycan sacculus of *Escherichia coli* K-12. Can. J. Microbiol. **30**, 204–211 (1984). doi:10.1139/m84-031
39. W. Bai, K. Zhao, K. Asami, Effects of copper on dielectric properties of *E. coli* cells. Colloids Surf. B **58**, 105–115 (2007). doi:10.1016/j.colsurfb.2007.02.015
40. R. Nandakumar, C.E. Santo, N. Madayiputhiya et al., Quantitative proteomic profiling of the *Escherichia coli* response to metallic copper surfaces. Biometals **24**, 429–444 (2011). doi:10.1007/s10534-011-9434-5
41. A.E. Pelling, Y.N. Li, W.Y. Shi et al., Nanoscale visualization and characterization of *Myxococcus xanthus* cells with atomic force microscopy. Proc. Natl. Acad. Sci. U.S.A. **102**, 6484–6489 (2005). doi:10.1073/pnas.0501207102